

Instability of a Bose-Einstein Condensate with Attractive Interaction

Antonios Eleftheriou and Kerson Huang

Department of Physics and Center for Theoretical Physics

Massachusetts Institute of Technology

Cambridge, MA 02139, USA

(October 1, 2018)

03.75.Fi, 42.65.Jx, 32.80.Pj

MIT-CTP #2886

We study the stability of a Bose-Einstein condensate of harmonically trapped atoms with negative scattering length, specifically ${}^7\text{Li}$. Our method is to solve the time-dependent nonlinear Schrödinger equation numerically. For an isolated condensate, with no gain or loss, we find that the system is stable (apart from quantum tunneling) if the particle number N is less than a critical number N_c . For $N > N_c$, the system collapses to high-density clumps in a region near the center of the trap. The time for the onset of collapse is on the order of 1 trap period. Within numerical uncertainty, the results are consistent with the formation of a “black hole” of infinite density fluctuations, as predicted by Ueda and Huang [16]. We obtain numerically $N_c \approx 1251$. We then include gain-loss mechanisms, i.e., the gain of atoms from a surrounding “thermal cloud”, and the loss due to two- and three-body collisions. The number N now oscillates in a steady state, with a period of about 145 trap periods. We obtain $N_c \approx 1260$ as the maximum value in the oscillations.

I. INTRODUCTION AND SUMMARY

Bose-Einstein condensation has been observed in magnetically trapped dilute vapors of the alkali elements ${}^{87}\text{Rb}$ [1], ${}^{23}\text{Na}$ [2], ${}^7\text{Li}$ [4], and ${}^1\text{H}$ [3]. At the nanodegree temperatures of these experiments, the systems would have frozen solid long ago were they in free space. In the confining trap, however, zero-point motion keeps the atoms apart, and the systems remain gaseous. The case of ${}^7\text{Li}$ is special, however, in that the interatomic interaction is predominantly attractive, as indicated by a negative scattering length. Thus, the condensate in ${}^7\text{Li}$ should be less stable than the other cases. The purpose of this paper is to study the nature of the instability, its onset, and manifestations.

The object of study is the condensate wave function $\psi(\mathbf{r}, t)$, which gives the probability amplitude for annihilating one particle in the condensate at \mathbf{r} at time t . We use the time-dependent Gross-Pitaevskii (GP) equation, or nonlinear Schrödinger equation (NLSE), which corresponds to a mean-field approximation:

$$i\hbar\frac{\partial\psi}{\partial t} = \left[-\frac{\hbar^2}{2m}\nabla^2 + V(r) - U_0|\psi|^2 \right] \psi$$
$$U_0 = \frac{4\pi\hbar^2|a|}{m} \tag{1}$$

where a is a negative scattering length, and the external potential is taken to be harmonic:

$$V(r) = \frac{1}{2}m\omega^2 r^2 \quad (2)$$

This defines a characteristic length d_0 , the width of the unperturbed ground-state wave function:

$$d_0 = \sqrt{\frac{\hbar}{m\omega}} \quad (3)$$

The number of condensate particles enters through the normalization

$$N = \int d^3r |\psi|^2 \quad (4)$$

which is a constant of the motion. Another constant of the motion is the Hamiltonian

$$H = \int d^3r \left[-\frac{\hbar^2}{2m} \psi^* \nabla^2 \psi + V(r) \psi^* \psi - \frac{U_0}{2} (\psi^* \psi)^2 \right] \quad (5)$$

The parameters used in ^7Li experiments correspond to [4]

$$\begin{aligned} a &= -1.45 \text{ nm} \\ d_0 &\approx 3.16 \text{ } \mu\text{m} \\ \omega &\approx 908 \text{ s}^{-1} \end{aligned} \quad (6)$$

where ω is taken to be approximately equal to the geometric mean of the three circular frequencies of the experimental trap. Equation (1) does not take into account the coupling between the condensate and the “thermal cloud” of uncondensed atoms, nor does it describe the loss of atoms from the trap due to collisions. These effects will be considered later.

In free space, the NLSE with attractive interactions has an instability known in plasma physics as “self-focusing” [5], whereby the initial wave function develops a singularity in finite time, corresponding to a local collapse to a state of infinite density. In an external trap, however, the ground state is apparently stable, as long as N is not too large, as indicated by variational calculations using a Gaussian trial wave function [6]. The width of the Gaussian narrows with increasing N , and collapses to zero at some critical value N_c . This conclusion is borne out by other studies [7–11]. In particular, Kim and Zubarev obtain an exact upper bound for N_c , which for a Gaussian wave function gives

$$N_c \leq 0.671 \frac{d_0}{|a|} \quad (7)$$

Ueda and Leggett [9] obtain the upper bound in a variational calculation. For the ^7Li parameters (6), this formula gives $N_c \leq 1463$. In the numerical calculations described later, we obtain

$$N_c = 0.574 \frac{d_0}{|a|} \quad (8)$$

or $N_c = 1251$ for the ${}^7\text{Li}$ parameters. This number becomes slightly larger when gain and loss effects are taken into account.

Actually, even ignoring collisional loss, the condensate is only metastable for $N < N_c$, for it can decay via quantum tunneling. This effect is not described by the NLSE, although an approximate decay amplitude can be obtained by continuation of the NLSE to imaginary time. Kagan et al. [12] estimated the amplitude by calculating an overlap integral between initial and final states represented by Gaussian wave functions, and obtained $(d_f/d_i)^{3N/2}$, where d_i and d_f are respectively the widths of the initial and final wave functions. Through numerical calculations, Shuryak [13] found that the decay rate is proportional to $\exp[-\text{const.}(N_c - N)]$. Stoof [14] wrote down a WKB formula for the decay rate, but did not explicitly evaluate it. Using variational wave functions, Ueda and Leggett [9] obtained a rate proportional to $\exp[-\text{const.}(N_c - N)^{5/4}]$. These estimates indicate that the tunneling probability is negligible unless $N \approx N_c$. However, the WKB approximation breaks down in this neighborhood, and reliable calculations become difficult. In experimental terms, it is also difficult to observe tunneling in the present system, because the effect is masked by collisional loss, especially near $N = N_c$ [15]. For these reasons, we shall not calculate the tunneling amplitude in this paper; but we will give a qualitative discussion of the phenomenon, in as far as it pertains to the instability of the system.

Ueda and Huang [16] formulated an approach to the stability problem, including tunneling, in terms of the Feynman path integral for a transition amplitude. In a saddle-point approximation to the path integral, one obtains the NLSE as the saddle-point condition, whose continuation into imaginary time yields the tunneling amplitude. Starting with a Gaussian initial wave function, they assume that it remains Gaussian, in order to analyze the problem analytically. In this ‘‘Gaussian approximation’’, it was found that, as soon as $N > N_c$, the system begins to collapse locally, in a region at the center of the trap. The size of this region grows as N increases. By putting the NLSE in hydrodynamic form, one can see that the pressure becomes negative inside this ‘‘black hole’’, and, consequently, there would be infinite density fluctuations.

In the present work, we remove the Gaussian approximation by performing numerical calculations. We verify that the picture presented by Ueda and Huang is correct. For $N > N_c$, a ‘‘black-hole’’ does appear at the center of the trap, within which the density has sharp local maxima, whose heights grow as the grid size for the numerical computation is decreased. This is consistent with the expectation that the density becomes divergent in the continuum limit. Finally, we take into account gain and loss mechanisms by adding phenomenological terms to the NLSE. We are able to study in some detail the growth-collapse cycles of the condensate, as anticipated in earlier work [17,18].

II. TUNNELING AND COLLAPSE

To give an overview of the mechanisms for instability, we think of the condensate wave function at each spatial point as a ‘‘coordinate,’’ which moves in an effective potential, consisting of the last two terms in the Hamiltonian (5), plus fluctuation corrections arising from the term $\psi^*\nabla^2\psi$. The system is classically stable when this motion is bounded at all spatial points. We immediately see that the attractive interaction term $-\frac{U_0}{2}(\psi^*\psi)^2$ can lead

to instability, for it decreases without bound when the density increases. The question is whether there is an energy barrier guarding against the free fall.

A precise definition for the effective potential can be modeled after that for a spatially uniform system in quantum field theory [19]. For a qualitative description, however, it is much simpler to use the ‘‘Gaussian approximation’’ introduced by Ueda and Huang [16], where we assume that the wave function is Gaussian, given by its initial form

$$\psi_0(r) = C_0 \exp(-r^2/d^2) \quad (9)$$

where

$$C_0 = \pi^{-3/4} d^{-3/2} \sqrt{N} \quad (10)$$

We introduce a width parameter α by putting

$$d = \frac{d_0}{\sqrt{\alpha}} \quad (11)$$

Thus, $\alpha = 1$ corresponds to the ground-state eigenfunction of the harmonic oscillator. With this, we have

$$-\frac{\hbar^2}{2m} \nabla^2 \psi_0 = \chi(r) \psi_0 \quad (12)$$

where

$$\chi(r) = \frac{\hbar^2}{2m d_0^2} \left[3\alpha - \left(\frac{r}{d_0} \right)^2 \alpha^2 \right] \quad (13)$$

and in this approximation the effective potential is

$$\Omega_r(\psi) = [V(r) + \chi(r)] |\psi|^2 - \frac{U_0}{2} |\psi|^4 \quad (14)$$

This is depicted on the right panel of Fig. 1 for different r . There is an energy barrier with height

$$W_r = \frac{1}{U_0} [V(r) + \chi(r)]^2 \quad (15)$$

which is nonzero at $r = 0$, because $\chi(0) \neq 0$. At large $|\psi|$ the effective potential tends to $-\infty$. In reality, of course, the NLSE ceases to be valid somewhere along the drop, for other physical effects, such as solidification, come in.

A typical initial wave function $\psi_0(r)$ is shown on the left panel of Fig. 1. At a given r , we can measure the wave function on the left panel, and transfer it to the horizontal axis on the right panel. If it lands to the left of the barrier maximum for the particular r , then the system at that point is classically stable, but can decay via quantum tunneling as indicated by the classically forbidden path $A \rightarrow B$. If it lands to the right, the system at that r will rapidly collapse to a state of high density.

Since $\psi_0(r)$ has a maximum at $r = 0$ with value proportional to \sqrt{N} , the system may only decay via tunneling at any r , if it is classically stable at $r = 0$. Otherwise, the system in a region about $r = 0$ will rapidly collapse. The condition for stability against collapse is therefore

$$\Omega_0(\psi_0(0)) < W_0 \quad (16)$$

which corresponds to $N < N_c$, with

$$N_c = \frac{3}{8} \sqrt{\frac{\pi}{\alpha}} \frac{d_0}{|a|} = \frac{0.665}{\sqrt{\alpha}} \frac{d_0}{|a|} \quad (17)$$

The time for the onset of local collapse is expected to be greater than the time needed to establish a quasi-stationary initial wave function. Thus, α should correspond to the best Gaussian approximation to that wave function. This expectation is verified by numerical calculations described below, which also show that the Gaussian approximation is very good, up to the onset of collapse. Of course, α ceases to have meaning once the collapse begins, for $N > N_c$. The numerical calculations for $N = 1248$, which is just below N_c , give

$$\alpha = 1.79 \quad (18)$$

As mentioned earlier, we will not calculate the tunneling amplitude in this paper, but concentrate on numerical solutions of the NLSE in real time.

III. STATIONARY STATE

We seek spherically symmetric solutions to the NLSE (1), for the parameters (6) for the ${}^7\text{Li}$ experiments. For convenience we put

$$\psi(r, t) = \sqrt{\frac{N}{4\pi d_0}} \frac{u(r, t)}{r} \quad (19)$$

with the boundary condition $u(0) = 0$, and the normalization condition

$$\frac{1}{d_0} \int_0^\infty dr |u(r, t)|^2 = 1 \quad (20)$$

From now on, we shall measure distance in units of d_0 , and time in units of $2\omega^{-1}$. To do this without introducing new symbols for dimensionless distance and time, we formally put $d_0 = \omega/2 = 1$. The NLSE (1) then takes the form

$$i \frac{\partial u}{\partial t} = \left(-\frac{\partial^2}{\partial r^2} + r^2 - \frac{2G|u|^2}{r^2} \right) u \quad (21)$$

where

$$G = \frac{N|a|}{d_0} = \frac{N}{2180} \quad (22)$$

The initial condition with Gaussian form is

$$u(r, 0) = u_0 r \exp\left(-\frac{1}{2}\alpha r^2\right) \quad (23)$$

where

$$u_0 = 2\pi^{-1/4}\alpha^{3/4} \quad (24)$$

We calculate u numerically as a complex function, using an implicit difference equation algorithm due to Goldberg et al. [20].

To find out how various initial states relax to a stationary state, we first solve the equation with an initial wave function uniform within a certain radius, and zero outside. For $N = 1142$, which is somewhat below the critical number, the time development is shown in Fig. 2(a). We see that the modulus $r|\psi|$ appears to be Gaussian-like, except for small local fluctuations, after only about one-hundredth of an oscillator cycle. In Fig. 2(b), we start with a Gaussian with $\alpha = 1$, with the same N . This corresponds to the stationary wave function in the absence of interatomic interaction. In a few oscillator cycles, the width narrows to a stationary value. If we initially choose α near the stationary value, the location of the peak of $r|\psi|$ will slowly oscillate about some mean position. Fig. 2(c) shows the case when the ratio of the standard deviation to the mean of the peak location is minimized. This corresponds to $\alpha = 1.48$, for this choice of N . The wave function in this case is sensibly stationary, and the Gaussian approximation is good.

In Fig. 3, we plot the ratio of the standard deviation to the mean of the peak location for $N = 1248$ (just below critical) against α , and exhibit the minimum at $\alpha = 1.79$, as quoted earlier in (18). For a quantitative measure of how good the Gaussian approximation is, we calculate the absolute value of the overlap between $u(r, t)$ and $u(r, 0)$ and find that it lies between 1 and 0.9795, with an average of 0.9906, for t between 0 and 50 (t in units of $2\omega^{-1}$).

IV. LOCAL COLLAPSE

To find N_c , we examine the time development for different N , to look for the onset of local collapse. The signature of the collapse is the occurrence of a minimum in the wave function within a small distance from the origin as shown in Fig. 4 for $\alpha = 1.79$ and $N = 1308$. The initial wave function is stationary for a while, but begins to narrow after $t \approx 0.2$ (Fig. 4(a)), and a dip occurs at $t \approx 0.7$ (Fig. 4(b)), at $r \approx 2.3$, which describes the implosion of a shell of particles at that radius. The first local minimum moves inwards with time and it eventually gets very close to $r = 0$, at $t \approx 0.9$, as shown in Fig. 4(c). The density in the inner region can grow only by taking particles from the outside, since the number of particles is conserved. An examination of the phase of the wave function, whose gradient gives the superfluid velocity, shows that the superfluid velocity has a peak at the dip, and is directed inward, as we expect from the continuity equation. Thus, qualitatively, the onset of collapse happens on a time scale an order of magnitude greater than that for the establishment of the initial wave function, and it is initiated by a sudden inward rush of particles from a finite distance from the center. This signals the formation of a “black hole”, as suggested by Ueda and Huang [16].

After the onset of collapse, the density in the black hole increases rapidly, as indicated in Fig. 4(c). The increase is fueled by particles drawn from throughout the outer region, but the density outside does not decrease uniformly. Instead, there are ripples of small implosions. This is illustrated in the 3D plot of Fig. 5, with $r|\psi|$ plotted above the r - t plane. The black hole formation is indicated by the sudden rise of $r|\psi|$ near the origin. The terrain is smooth before the rise, but very rough after that. The uneven bumps in the terrain are of course deterministic, but they are very sensitive to variations in the initial wave function, and in this sense they are random (see Fig. 6). The fact that the height of the plateau seems to remain constant in time is an artifact of the finite spatial grid size. The height appears to increase without bound in the continuum limit, as illustrated in Fig. 8.

To determine N_c more precisely, we plot the occurrence time of the first local minimum in the wave function within distance $r = 0.05$ from the origin, as a function of $G = N/2180$. This is done in Fig. 7, for a Gaussian initial wave function with $\alpha = 1.0$, and for an optimal Gaussian initial wave function with $\alpha = 1.79$. The results are as follows:

$$N_c = \begin{cases} 1145 & \text{(Gaussian initial state with } \alpha = 1.00) \\ 1251 & \text{(Gaussian initial state with } \alpha = 1.79) \end{cases} \quad (25)$$

which conforms to our expectation that the numbers are not very sensitive to initial conditions, because the time for the onset of collapse is long compared to the formation time of a quasi-stationary wave function.

In Fig. 8 we show the dependence of some of our results on the spatial grid size. The time for the onset of collapse appears to tend to a finite limit when the grid size approaches zero, but the height of a peak in the collapsed region seems to grow without bound, faster than $(\text{grid size})^{-1}$. This is consistent with the expectation that density fluctuations become divergent in the continuum limit.

V. GROWTH-COLLAPSE CYCLES

We have ignored gain-loss mechanisms so far, because we wanted to understand various effects one at a time. Now we shall take them into account, and make the problem more realistic.

In the experimental situation, the condensate in the trap can exchange atoms with an uncondensed “thermal cloud”, which contains far more atoms than the condensate. Equilibrium is reached when the chemical potentials equalize. The equilibrium fraction of condensate to “cloud” atoms is determined by the temperature. The kinetic equations governing the approach to equilibrium are quite intricate, and a subject of ongoing research [21]. We shall use a phenomenological gain equation based on a fit to data [22]:

$$\frac{dN}{dt} = c_0 N \left[1 - \left(\frac{N}{N_{\text{eq}}} \right)^{0.4} \right] \quad (26)$$

where N_{eq} is the equilibrium number of atoms in the condensate, with

$$c_0 = f\gamma = f\sqrt{8}\zeta(3/2)\gamma_{\text{el}}(15G_{\text{eq}})^{0.4} \frac{\hbar\omega}{k_B T} \quad (27)$$

where γ_{el} is the elastic scattering rate, which is approximately equal to 1 s^{-1} for the conditions of the experiment of Ref. [4] and $\zeta(3/2) \approx 2.612$. f is a phenomenological factor to reconcile the above theoretical prediction for γ with the experimental results for the repulsive case [22]. In our runs we used $f = 5.75$ and $T = 300 \text{ nK}$, while G_{eq} was taken to be equal to the critical value of G , i.e. about 0.574. Assuming $N/N_{\text{eq}} \ll 1$, we ignored the second term in the bracket. The main loss mechanisms are two- and three-body collisions [23] described by the following equation:

$$\begin{aligned} \frac{dn}{dt} &= -c_1 n^3 - c_2 n^2 \\ c_1 &= 2.6 \times 10^{-28} \text{ cm}^6/\text{s} \\ c_2 &= 1.2 \times 10^{-14} \text{ cm}^3/\text{s} \end{aligned} \quad (28)$$

where n is the particle density in the condensate. Adding the gain and loss terms, we have an extended NLSE, which reads, in units such that $d_0 = 2\omega^{-1} = 1$,

$$i \frac{\partial u}{\partial t} = \left(-\frac{\partial^2}{\partial r^2} + r^2 - \frac{2G|u|^2}{r^2} \right) u + i \left(\gamma_0 - \gamma_1 \frac{G^2|u|^4}{r^4} - \gamma_2 \frac{G|u|^2}{r^2} \right) u \quad (29)$$

where

$$\begin{aligned} \gamma_0 &= 2.6 \times 10^{-3} \\ \gamma_1 &= 8.3 \times 10^{-6} \\ \gamma_2 &= 7.2 \times 10^{-5} \end{aligned} \quad (30)$$

In Ref. [18], the value of γ_1 is taken to be of order 10^{-3} , which differs considerably from ours.

With the new equation, we find that the initial conditions become quite irrelevant. The number of particles quickly settle into a steady-state oscillation whose peak value defines the critical particle number in the new context. This is shown in Fig.9, with:

$$N_c \approx 1260 \quad (31)$$

The mean number of atoms is approximately 735, and the period of the oscillation is

$$\tau \approx \frac{917}{\omega} = 1.01 \text{ s} \quad (32)$$

The long time scale of the oscillations explains why they are insensitive to initial conditions. We have extended the calculations to the longest evolution time practicable, and found that, with a constant supply of particles, N oscillates in a steady state for at least 1.44×10^4 trap cycles, or 100 seconds. These results are comparable with those obtained by Hulet et al. [17], except that, in contrast to our case, N collapses to zero in that calculation.

ACKNOWLEDGMENT

This work is supported in part by a DOE cooperative agreement DE-FC02-94ER40818.

REFERENCES

- [1] M. H. Anderson, J. R. Ensher, M. R. Mathews, C. E. Wieman, and E. A. Cornell, *Science* **269**, 198 (1995).
- [2] K. B. Davis, M.-O. Mewes, M. R. Andrews, N. J. van Druten, D. S. Durfee, D. M. Kurn, and W. Ketterle, *Phys. Rev. Lett.* **75**, 3969 (1995).
- [3] D. G. Fried, T. C. Killan, L. Willmann, D. Landhuis, S. C. Moss, D. Kleppner, and T. J. Greytak, *Phys. Rev. Lett.* **81**, 3811 (1998).
- [4] C. C. Bradley, C. A. Sackett, J. J. Tollett, and R. G. Hulet, *Phys. Rev. Lett.* **75**, 1687 (1995); C. C. Bradley, C. A. Sackett, and R. G. Hulet, *Phys. Rev. Lett.* **78**, 985 (1997).
- [5] V. E. Zakharov and V. S. Synakh, *Zh. Eksp. Teor. Fiz.* **68**, 940 (1975). [*Sov. Phys. JETP* **41**, 465 (1976).]
- [6] G. Baym and C. J. Pethick, *Phys. Rev. Lett.* **76**, 6 (1996).
- [7] P. A. Ruprecht, M. J. Holland, K. Burnett, and M. Edwards, *Phys. Rev. A* **51**, 4704 (1995).
- [8] F. Dalfovo and S. Stringari, *Phys. Rev. A* **53**, 2477 (1996).
- [9] M. Ueda and A. J. Leggett, *Phys. Rev. Lett.* **80**, 1576 (1998).
- [10] Y. E. Kim and A. L. Zubarev, *Phys. Lett. A* **246**, 389 (1998).
- [11] M. Wadati and T. Tsurumi, *Phys. Lett. A* **247**, 287 (1998).
- [12] Yu. Kagan, G. Shlyapnikov, and J. Walraven, *Phys. Rev. Lett.* **76**, 2670 (1996).
- [13] E. Shuryak, *Phys. Rev. A* **54**, 3151 (1996).
- [14] H. T. C. Stoof, *J. Stat. Phys.* **87**, 1353 (1997).
- [15] D. M. Stamper-Kurn, H.-J. Miesner, A. P. Chikkatur, S. Inouye, J. Stenger, and W. Ketterle, *Phys. Rev. Lett.* **83**, 661 (1999) reported observation of tunneling of two different condensates through each other.
- [16] M. Ueda and K. Huang, *Phys. Rev. A* (in press); cond-mat/9807359.
- [17] C. A. Sackett, H. T. C. Stoof, and R. G. Hulet, *Phys. Rev. Lett.* **80**, 2031 (1998).
- [18] Yu. Kagan, A. E. Muryshev, and G. V. Shlyapnikov, cond-mat/9801168 (16 Jan 1998).
- [19] See, for example, K.Huang, *Quantum Field Theory*, (Wiley, New York, 1998), Sec.15.7.
- [20] A. Goldberg, H. M. Schey, and J. L. Schwartz, *Am. J. Phys.* **35**, 177 (1967).
- [21] T. R. Kirkpatrick and J. R. Dorfman, *Phys. Rev. A* **28**, 2576 (1985); D. W. Snoke and J. P. Wolfe, *Phys. Rev. B* **39**, 4030 (1989); D. V. Semikoz and I. I. Tkachev, *Phys. Rev. Lett.* **74**, 3093, (1995); C. W. Gardiner, M. D. Lee, R. J. Ballagh, M. J. Davis, and P. Zoller, cond-mat/9806295 (24 Jun 1998); T. Nikuni, E. Zaremba, and A. Griffin, cond-mat/9812320 (18 Dec 1998).
- [22] H.-J. Miesner, D. M. Stamper-Kurn, M. R. Andrews, D. S. Durfee, S. Inouye, W. Ketterle, *Science*, **279**, 1005, (1998).
- [23] R. J. Dodd, M. Edwards, C. J. Williams, C. W. Clark, M. J. Holland, P. A. Ruprecht, and K. Burnett, *Phys. Rev. A* **54**, 661 (1996).

FIGURES

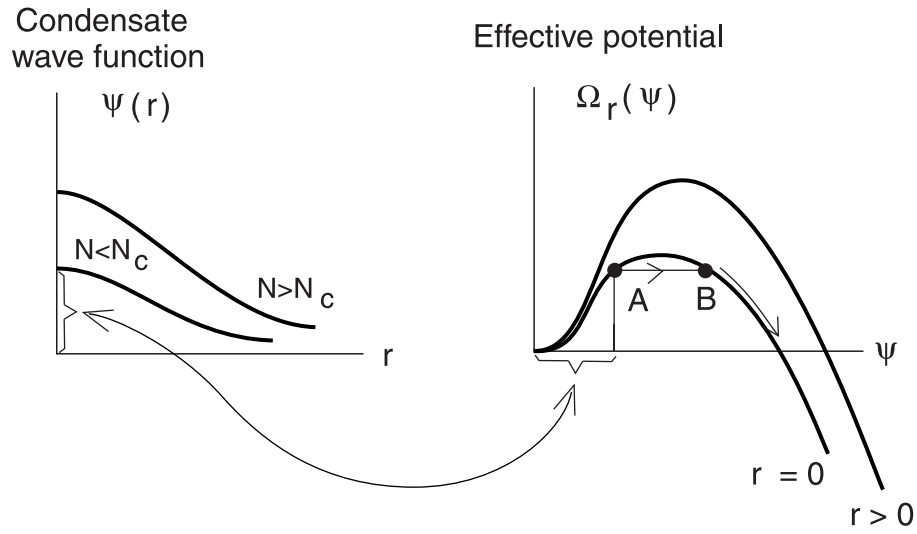


FIG. 1. Transfer a local value of the wave function from the left panel to the horizontal axis on the right. If it lands to the left of the potential barrier, the local system is classically stable, but can decay via tunneling, as indicated by the path $A \rightarrow B$. If it lands to the right, the local system will rapidly collapse towards a state of infinite density.

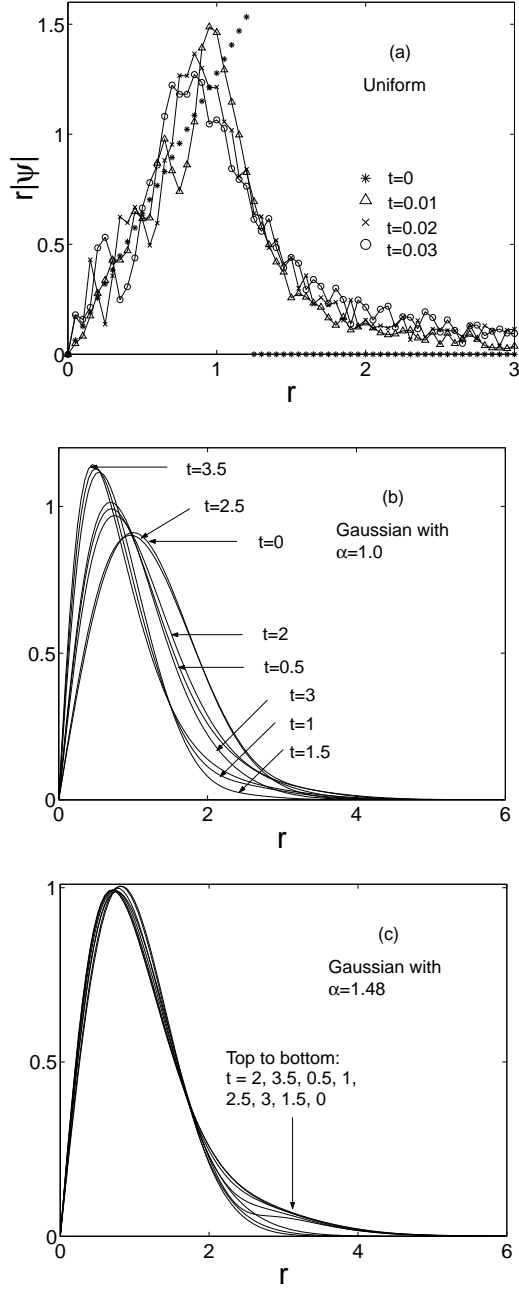


FIG. 2. Time development of the condensate wave function. The time steps are given in units of $2\omega^{-1}$, where ω is the circular frequency of the external harmonic trap. The number of particles is $N = 1142$ (i.e. $G = N/2180 = 0.524$), which is the highest particle number for which a Gaussian initial wave function with $\alpha = 1.0$ is stable. (a) An initially uniform wave function tends to Gaussian form, except for local fluctuations, after a few time steps. (b) For an initial unperturbed Gaussian wave function with width d_0 , the width narrows to a stationary value after a few time steps. (c) Starting from a Gaussian with width $d_0/\sqrt{1.48}$ gives a sensibly stationary wave function.

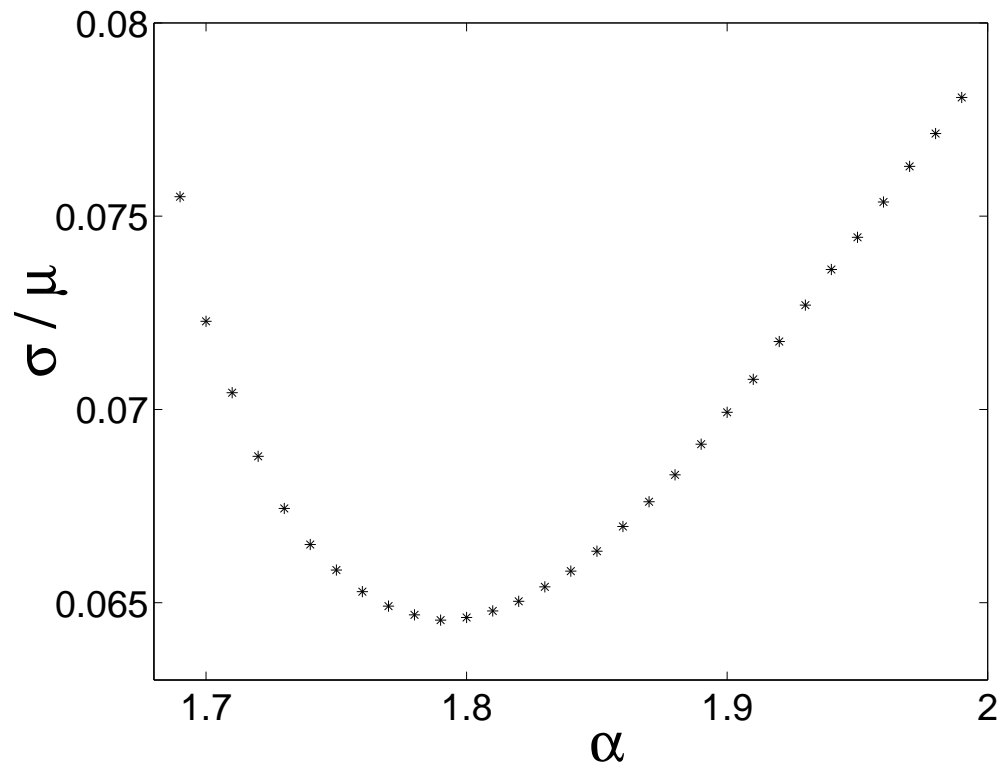


FIG. 3. Determining the best width $d = d_0/\sqrt{\alpha}$ of the initial Gaussian wave function $\psi_0(r)$, for $N = 1248$ ($G = 0.5725$), by minimizing the ratio of the standard deviation of the peak location to the mean peak location of $|u(r, t)|$. The minimum occurs at $\alpha = 1.79$.

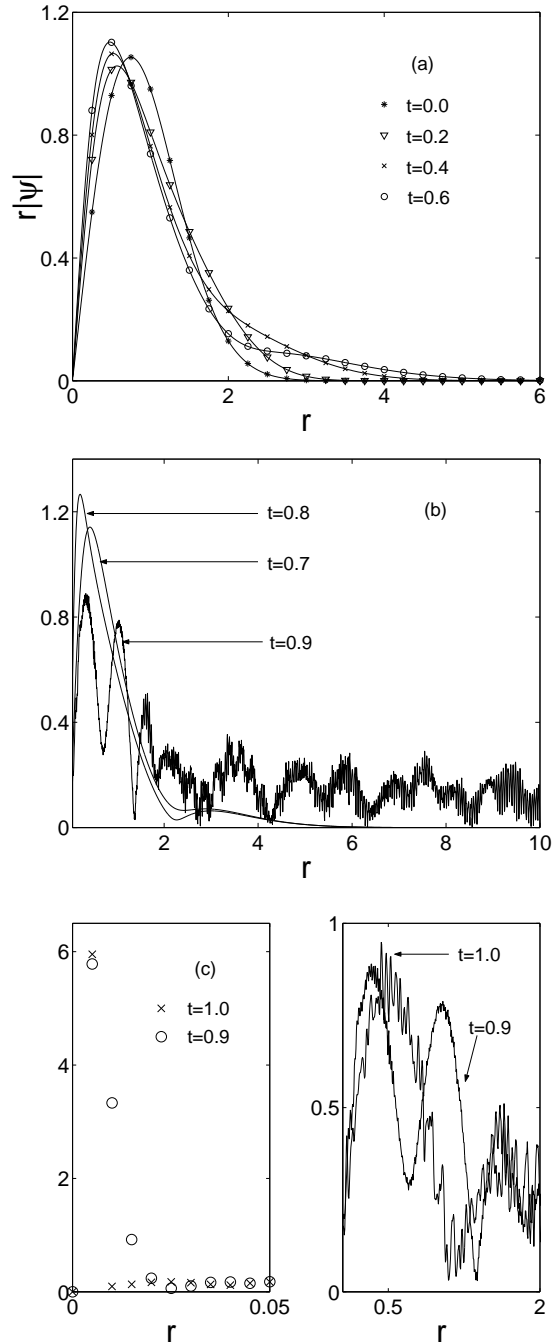


FIG. 4. Time development of unstable case, with $N = 1380$. (a) The wave function begins to narrow after $t \approx 0.2$. (b) The onset of collapse is signaled by the first occurrence of a dip (local minimum) in the wave function within a small distance from the origin, which indicates that a shell of particles begins to implode. The dip first appears at $t \approx 0.7$ and moves quickly towards $r = 0$. After the onset, the collapse continues by drawing in particles from all distances, in ripples of implosive flow. In this figure the first 10 grid points ($r \leq 0.05$) were cut off for clarity. (c) The first local minimum of the wave function is now at less than $r = 0.05$. The wave function becomes more ragged as time goes on. Because of the finiteness of the grid the density at the center remains finite.

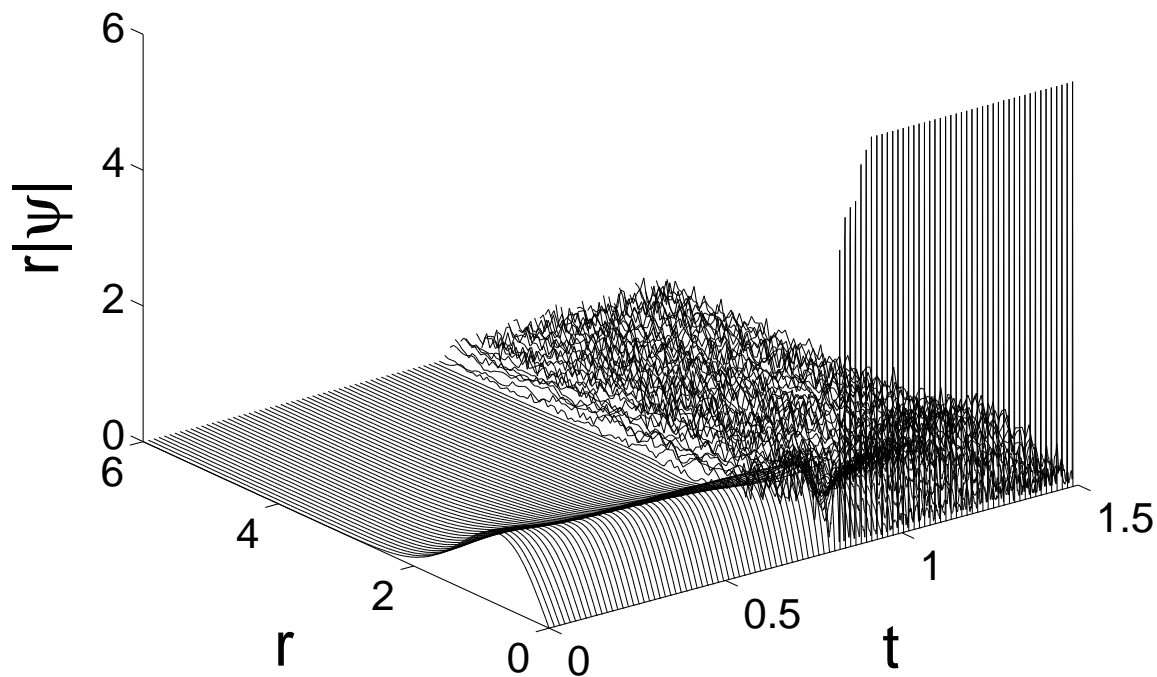


FIG. 5. Space-time behavior of the wave function of Fig. 4 in a 3D plot. The black hole formation is indicated by a sudden emergence of the high plateau. After that time, the terrain in the plain below the plateau becomes rough, indicating the ripples of implosive flow. As the spatial grid size tends to zero, the height of the plateau seems to increase without limit. (See Fig. 8.)

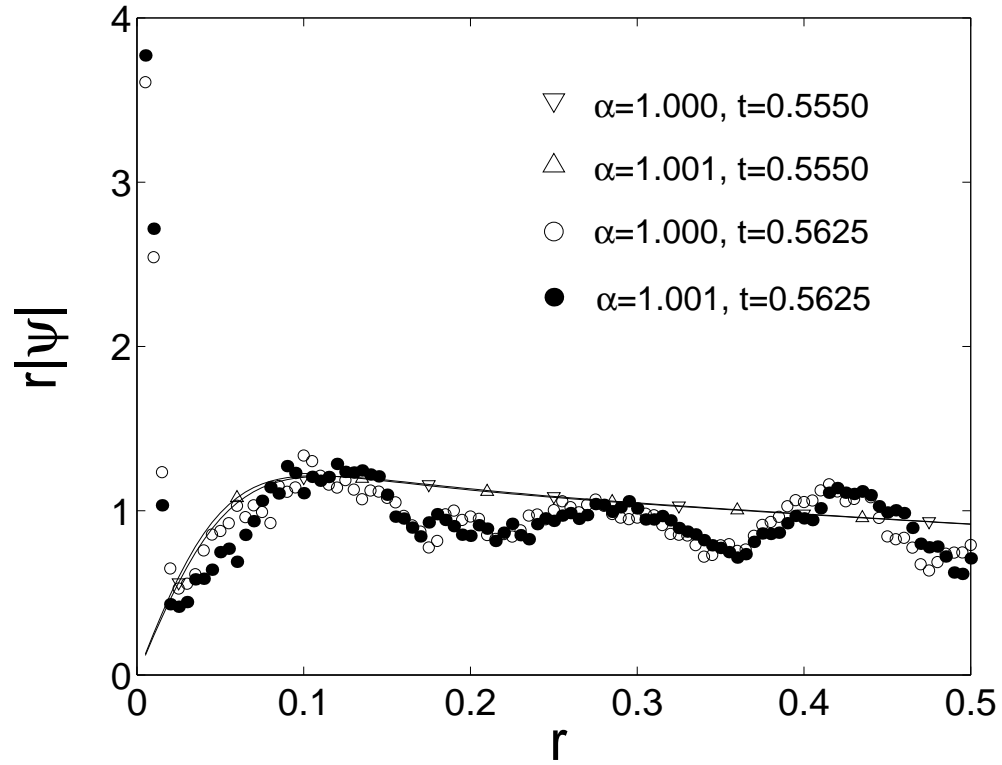


FIG. 6. Sensitivity of ripples to the initial conditions. We show the amplitude of the wave function just before and after the onset of the collapse for two nearly identical initial wave functions, Gaussians with $\alpha = 1$ and $\alpha = 1.001$. Notice that, before the collapse, the two wave functions practically coincide. However, once the collapse occurs, they diverge very quickly.

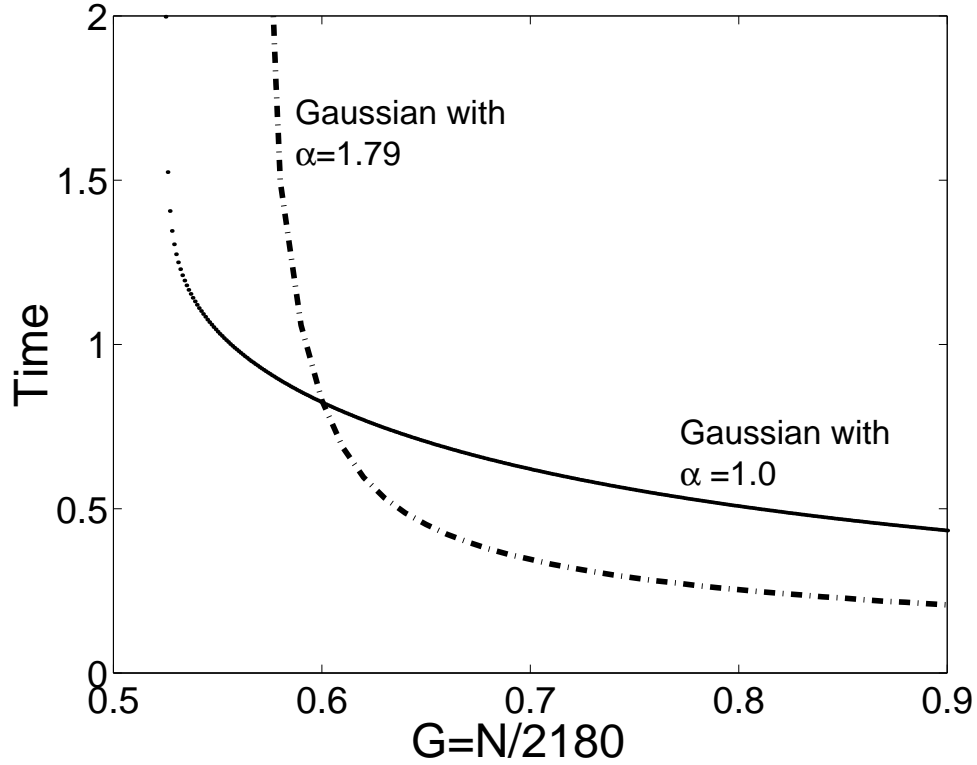


FIG. 7. Time for the onset of collapse *vs* $N/2180$. The two curves correspond to a Gaussian initial wave function with $\alpha = 1.0$ and to a Gaussian initial wave function with $\alpha = 1.79$. The critical number N_c is determined by the asymptote at which the time goes to infinity. We get $N_c = 1145$ ($G_c = 0.525$) when $\alpha = 1.0$ and $N_c = 1251$ ($G_c = 0.574$) when $\alpha = 1.79$. The results for the critical number are not very sensitive to the initial wave function.

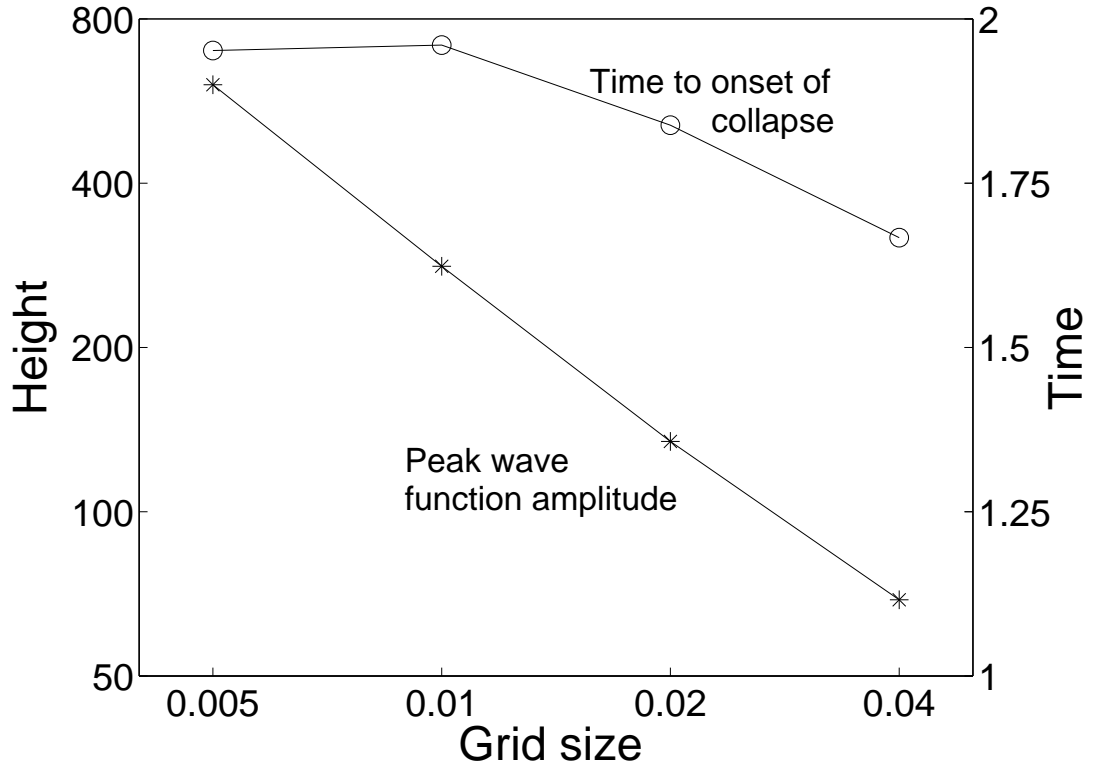


FIG. 8. Sensitivity of results on the spatial grid size, measured in units of d_0 . The initial wave function is Gaussian with $\alpha = 1.0$. Circles represent the time for the onset of collapse, which tends to a finite value in the continuum limit. Asterisks indicate the height of the peak of the square root of the density in the collapsed region. It appears to increase without limit as the grid size tends to zero. With the log-log axes used, the best linear fit has a slope of slightly less than -1 , which implies that the height of the peak increases faster than $(\text{grid size})^{-1}$ as the grid size goes to zero.

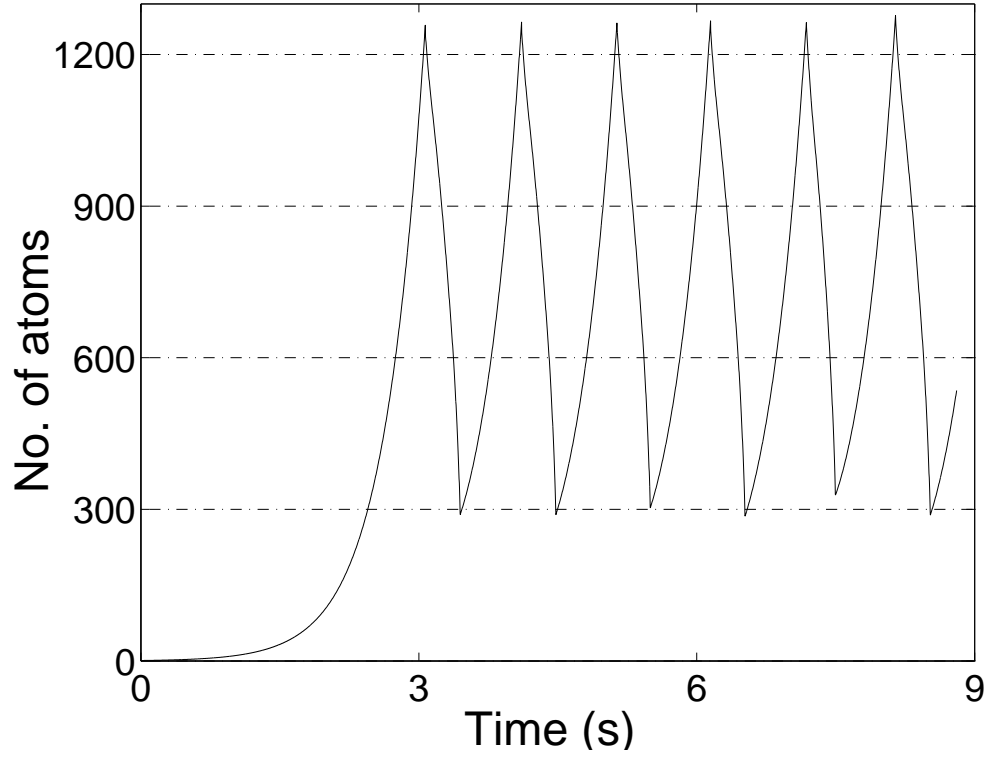


FIG. 9. Steady-state oscillation of the number of particles, when the condensate is fed by a “thermal cloud” and suffers loss through two- and three-body collisions. The peaks give $N_c \approx 1260$. The period of 1.01 s is much greater than the trap period of 7 ms. For this reason, initial conditions are irrelevant.